

Development of texture and texture gradient in Al-Cu-Li (2195) thick plate

K. E. CROSBY

Department of Mechanical Engineering, Louisiana State University, Baton Rouge, LA 70803, USA

R. A. MIRSHAMS

Department of Mechanical Engineering, Southern University, Baton Rouge, LA 70813, USA

S. S. PANG*

Department of Mechanical Engineering, Louisiana State University, Baton Rouge, LA 70803, USA

E-mail: mepang@me.lsu.edu

Texture resulting from micromechanical processing plays an important role in the anisotropy of materials. The determination of texture components is a useful way to present texture data. The types of components present in the texture of a material can be related to other material aspects including predictions of yield loci using polycrystal methods. Al-Cu-Li 2195 thick plate was cold rolled to produce various reductions in thickness. Texture analysis was performed on the various rolled materials at different positions through the thickness of the plates. The texture components are consistent among the various rolled specimens at equivalent thickness positions. A texture gradient is observed to exist through the plate thickness that may indicate other microstructural information about the alloy. This texture gradient evidences the effects of increasing amounts of deformation on texture intensity, texture components observed, and changing modes of deformation. © 2000 Kluwer Academic Publishers

1. Introduction

There have been numerous studies of the various Al-Li alloys [1–3]. It has been concluded that the various particles that form during natural and artificial aging provide barriers to dislocation motion during the micromechanical process of slip, which is the microstructural mode of deformation for most metallic materials. This impedance provides these materials with improved strength properties over conventional aluminum alloys while their various chemical compositions lead to lower densities than their conventional counterparts. For this reason, Al-Li alloys are of significant interest to the aerospace industries. Al-Li alloys are typically anisotropic and they exhibit strong textures. The texture or crystallographic orientation of a material is a measurement of the orientation of crystallographic planes in specific directions, namely the rolling, transverse, and normal directions of a sample.

Anisotropy of mechanical properties in different directions of measurement is a concern in the forming of metals into shapes and parts. It is tied into considerations of the yield locus. Various factors cause anisotropy in metals, including elongated grains [4], and the presence of second-phase precipitates [3, 5]. Researchers [6] agree that crystallographic textures or

preferred orientations resulting from thermomechanical treatment such as hot or cold rolling or stretching are most directly responsible for anisotropy in metal alloys. For Al-Li alloys, crystallographic texture may also have an indirect effect on anisotropy resulting from the heterogeneous distribution of the primary strengthening precipitates on specific habit planes. For these reasons, texture analysis is important for characterization of Al-Li materials.

Several sources [7–9] summarize the sources of texture and its effects on mechanical properties. In brief, texture arises from the rotation of material grains during the slip process when deformation occurs, which subsequently produces rotation of the crystallographic planes within the crystals comprising the grains. There is a limited number of slip systems available during slip, therefore the rotations occur towards a limited number of ‘end-points’ thus producing a deformation texture. Therefore the resulting texture depends on the nature of the imposed stress system and it reflects the symmetry of the forming operation.

Pole figures are graphical representations of texture. They are stereographic projections that show the distribution of particular crystallographic directions relative (usually) to material directions such as the rolling

* Author to whom all correspondence should be addressed.

direction (RD) and transverse direction (TD) in sheet materials. A pole figure exhibiting a typical rolling texture reflects the symmetry of the rolling process in that certain crystallographic planes are aligned parallel to the rolling plane and particular directions in these planes are parallel to the rolling direction. While pole figures are useful in the analysis of texture, they are merely qualitative representations of texture. On the other hand, the orientation distribution function (ODF) gives quantitative information about the spread of orientations throughout the texture of a material. As a full mathematical description, it can be applied objectively in understanding texture development and in the prediction of anisotropic properties. This paper covers the texture characteristics of an Al-Li plate with a discussion of the effects of deformation and aging on the texture and observed variations in texture at different locations through the plate thickness.

2. Experimental

2.1. Material

The Al-Cu-Li 2195 material used in this investigation was produced at Reynolds Metals Co. as 3.81 cm-thick plates in the T3 condition (heat treated and cold rolled); the weight percentages of the aluminum alloying elements are given in Table I. The as-received plate was cut into sections then solutionized in air for one hour at 540°C following with a water quench. Subsequently, the sections were additionally cold rolled to various thickness reduction percentages (0, 10, 20, and 30% reductions) to induce various amounts of deformation. This is of interest because the major strengthening precipitate, T_1 , forms preferably at the sites of dislocations, which are created during deformation. It is also of interest to observe what textural changes occur with additional rolling of this commercial product. Next, natural aging at room temperature for >1000 h and artificial aging at 180°C for 15 h were performed.

2.2. Describing through-thickness position

In order to obtain a general profile of the hardness through the thickness of the plate, hardness measurements were made at seven positions through the thickness of the plate as shown in Fig. 1. Rockwell B-scale measurements were carried out at a position near the plate surface, at the center of the plate, and at two positions between the center and the surface on both sides of the center. Assuming the characteristics of the plates to be symmetric about the center, the positions of the measurements were numbered from either plate surface starting at one, through four, at the plate center. Specifically, the distance from the surface to the measurements at position one was near 5% of the total thickness of the plate. The other measurements were

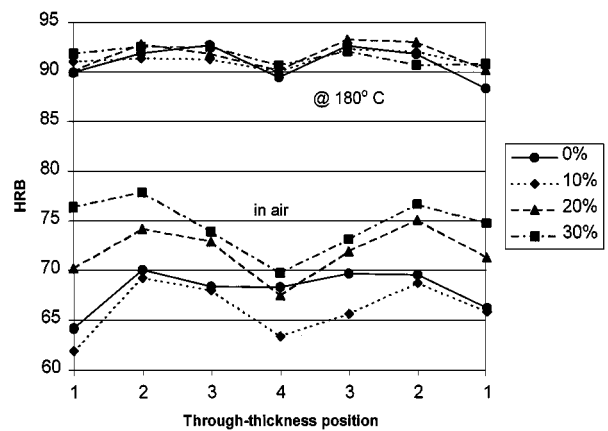


Figure 1 Through-thickness hardness variation of rolled and aged plates. Measurements performed with Rockwell hardness testing machine, B-scale with a 1/16 inch ball indenter.

spaced apart approximately 15% of the total plate thickness. A notation for through-thickness position may be assumed such that the position is described as a percentage of the total thickness, t , as measured from the plate surface. In this fashion, the following designation is given: position 1 = $0.05t$, position 2 = $0.2t$, position 3 = $0.35t$, and the center position 4 = $0.5t$. It is heretofore assumed that there is agreement within a reasonable variant of measured values from one side of the plate to the equivalent position on the other side. In hardness measurements, the variation from one side to the other was as low as approximately 0.05% and up to near 3.5% (\pm approximately 1%, due to the accuracy of the hardness tester). Subsequent tensile tests also support symmetry of characteristics about the plate center.

2.3. Selecting through-thickness location for samples

Through-thickness position for texture samples was chosen based on the hardness profile. Of most interest is the region where maximum hardness is measured. This lies within the region between positions $0.2t$ – $0.35t$. It is interesting to note that in the naturally aged condition, there is an average difference between the $0.2t$ and $0.35t$ positions, with the maximum generally at position $0.2t$, ranging from 1.28% to 5.08%, increasing with rolling percentage. On the other hand, in the artificially aged condition, the difference is negligible—at all rolling percentages the difference is under 1%. The following conclusions may be inferred from this: (1) the rolling process induces a deformation gradient that provides the largest shear within the $0.2t$ – $0.35t$ region, with a maximum at $0.2t$ and (2) the volume of T_1 formed with artificial aging is such that the increased hardness values within this region are basically the same. Therefore, texture specimens were obtained from the $0.2t$ position. Other samples were also obtained from the center of the plate, $0.5t$ (where hardness profiles showed the minimum values), for the artificial aged material with additional rolling for comparison.

TABLE I Al-Cu-Li 2195 alloy composition

Al	Cu	Li	Fe	Mg	Mn	Si	Ti	Zn	Zr	Ag
Balance	3.9	.9	.04	.33	<.01	.02	.02	.01	.14	.32

2.4. Texture measurement

For texture measurement, slices approximately 3 mm thick and 25 mm × 25 mm were cut from the bulk material. Polishing and etching of the surface was performed to remove the damage layer resulting from cutting. Fine polishing is not required for aluminum alloys because X-rays are able to penetrate the sample surface deeply enough to obtain accurate measurements. A Scintag Inc. X-ray goniometer with a Fe-K α radiation source was used for X-ray diffraction and measurement of diffraction intensities. The computer software, *popLA* [10] developed at Los Alamos National Laboratory (LANL), Los Alamos, New Mexico, was used to convert the recorded intensities for (111), (200), and (220) pole figures. Each pole figure is the average result of measurements from three like samples. These pole figures are in turn used for the calculation of the ODF plots using *popLA*.

Material processing and all texture measurements were performed at LANL within the Materials Science & Technology (MST) and Center for Materials Research (CMR) divisions. Aging treatments were performed at Louisiana State University's Materials Characterization Laboratory.

3. Results and discussion

The crystal orientations of rolling textures are usually characterized by the $\{hkl\}$ crystallographic plane parallel to the rolling plane and the $\langle uvw \rangle$ crystallographic direction parallel to the rolling direction [11]. From [9], a general orientation is described in the form $(hkl)[uvw]$. Textures are often approximated by varying amounts of ideal components with a statistical distribution around them [11]. The goal of depicting texture in terms of components is to reduce the representation of the orientation distribution into a small set of specific orientations [12] which describe a large number of crystallites present in the specimen. This may be

useful for relating the occurrence of particular texture components to certain material behavior. On such example is in the determination of yield surfaces, which is of interest when performing forming operations. Barlat and Richmond [13] predicted 2-dimensional yield loci in σ_1 - σ_2 stress space for ideal orientations including copper, brass, and Goss textures. According to their results, copper orientations produce more symmetrical yield loci with respect to the line of equibiaxial tension ($\sigma_1/\sigma_2 = 1$) compared to brass and Goss whereas the latter orientations produce distortion of the loci in the direction of σ_2 .

The names and orientations of some common texture components are defined in Table II. The stereographic projection of the $\{hkl\}\langle uvw \rangle$ direction into a reference sphere surrounding the crystallite may be used to define the orientation in spherical coordinates describing the location of the point of intersection of the projection with the sphere. Therefore, three Euler angles can define the orientation of a crystal and conversion to the $\{hkl\}\langle uvw \rangle$ form may be performed. Although they are all equivalent, several different definitions may be employed for such conversions, with as many different sets of symbols used to represent crystallite orientations. The traditional Bunge method [14] defines the orientation by three poles. The more recent Kocks form [15] which defines the orientation by a vector lying on the surface of the sphere is used for the ODFs presented in this paper. The orientations in Table II are expressed in both Bunge and Kocks notation and are illustrated as they appear in the ODFs shown in this paper using Kocks notation in Fig. 2.

Rolling textures tend to develop particularly around the copper, brass, and S orientations in aluminum alloys, whereas the recrystallization textures are usually identified by orientations such as Goss [13]. These ideal orientations may be predicted by using Sachs [16] or Taylor-type [17–20] theoretical modeling of polycrystal deformation. Aside from identifying the ideal orientation of intensity peaks, the method may be

TABLE II Ideal component orientations

Component	Orientation	Euler angles (degrees)					
		Bunge notation			Kocks notation		
		ϕ_1	Φ	ϕ_2	ψ	θ	ϕ
Copper (Cu)	$\{112\}\langle 111 \rangle$	90	35	45	0	35	45
S	$\{123\}\langle 634 \rangle$	59	37	63	149	37	27
Brass (Bs)	$\{110\}\langle 112 \rangle$	35	45	0	55	45	0
Goss	$\{110\}\langle 100 \rangle$	0	45	0	90	45	0

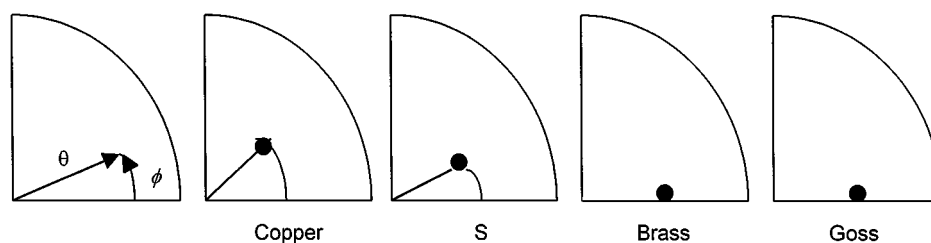


Figure 2 Locations of the ideal component orientations on the ODF as described using Kock's notation.

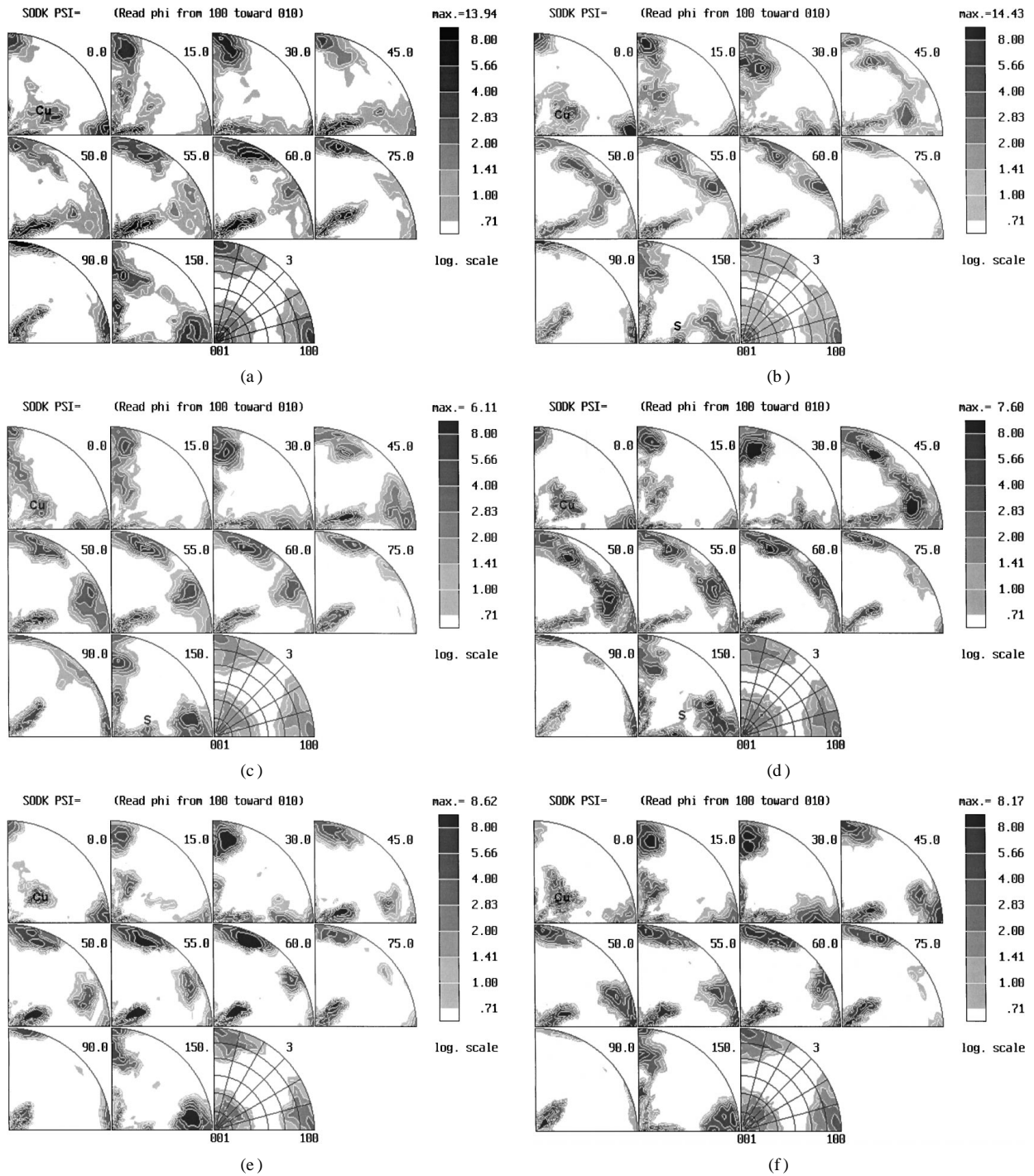


Figure 3 ODFs from $0.2t$ position (a) As-received, (b) 0% rolled-natural aged, (c) 10% rolled-natural aged, (d) 10% rolled-artificial aged, (e) 20% rolled-artificial aged, (f) 30% rolled-artificial aged. Texture components are denoted by: Cu—copper, and S.

extended to a more quantitative description including peak shape [21].

Fig. 3 exhibits the ODFs characterizing the $0.2t$ position of maximum strength (determined by hardness tests) through the thickness of the various rolled plates. Orientations in Figs 3 and 4 are described by Kocks Euler angle notation and are presented as slices of constant ψ with θ increasing radially and ϕ as the azimuthal angle. Intensities are indicated by the shaded gray-scale. The ODFs of the various samples tested do not differ significantly with variation of rolling percentage, except perhaps in value of maximum intensity. Fig. 4 shows ODFs calculated from the $0.5t$ (center) position of minimum hardness of the 10, 20, and 30%-artificially

aged plates. Comparison of Fig. 3d–f and Fig. 4 reveals a gradient through the thickness of the plate, which is in agreement with a similar study [22]. Changes in texture intensity and through-thickness texture gradients are reported [23] to affect yield locus shape and size.

The ODFs in Fig. 3 consist mainly of copper texture components with some S orientations, which diminish with increased deformation. Alternatively, the textures in Fig. 4 exhibit mainly a strong brass orientation. Flattening of grains during the rolling process leads to a shear misfit along the grain interfaces. Three shear misfit strains, ε_{xy} , ε_{xz} , and ε_{yz} , may be assumed to result from the shear forces producing the deformation. Using the Taylor relaxed constraints theory [24],

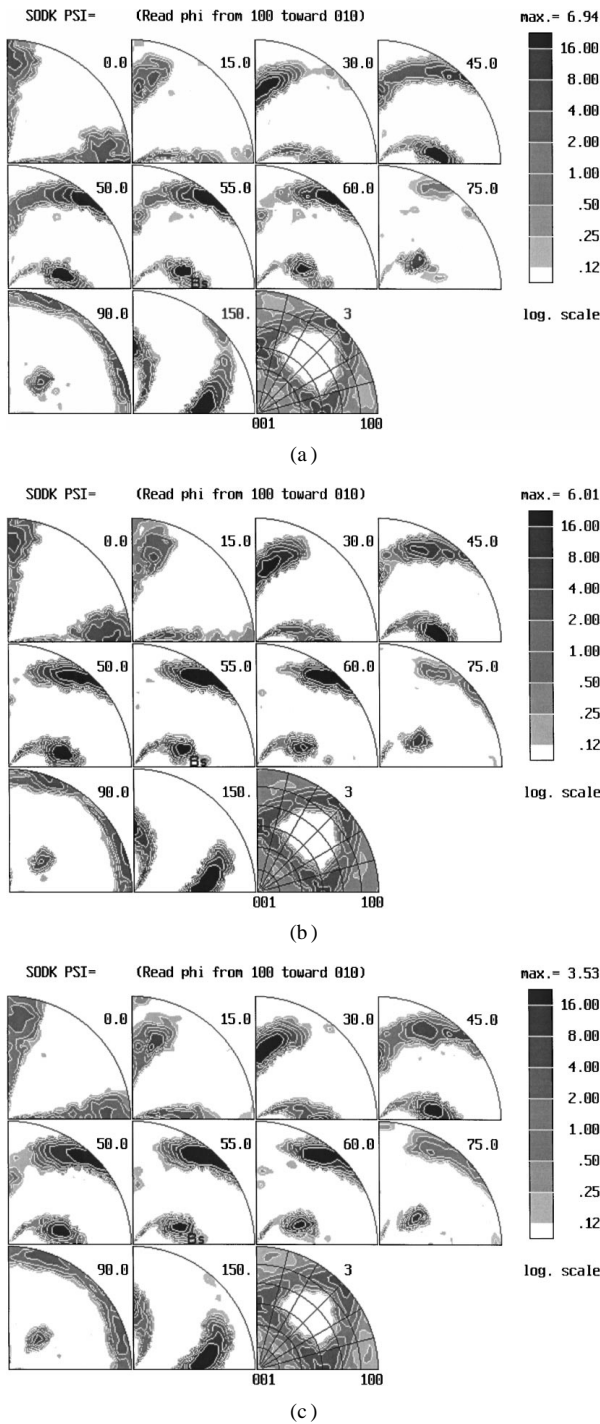


Figure 4 ODFs from 0.5t (center) position (a) 10% rolled-artificial aged, (b) 20% rolled-artificial aged, (c) 30% rolled-artificial aged. Texture components are denoted by: Bs—brass.

Mecking [25] predicts that when ε_{xy} and ε_{xz} are simultaneously released, as in the case of flat grains, the texture consists of two components, copper and S. By the same model, if ε_{yz} becomes freely adjustable, the brass component becomes prevalent. Because an unconstrained ε_{yz} is not consistent with flat grains, the effect is attributed to a characteristic termed “anisotropy of environment.” In this case, twinning occurs, promoting the $\{110\}\langle 112 \rangle$ brass orientation by reducing the constraints, and simultaneously removing the copper and S orientations from the texture. However, twinning is not expected to occur in aluminum alloys due to high stacking fault energy.

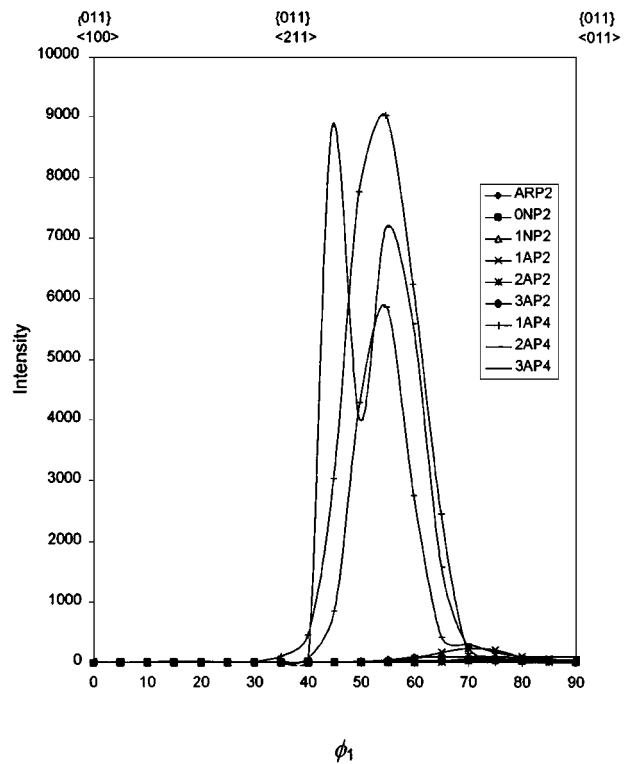
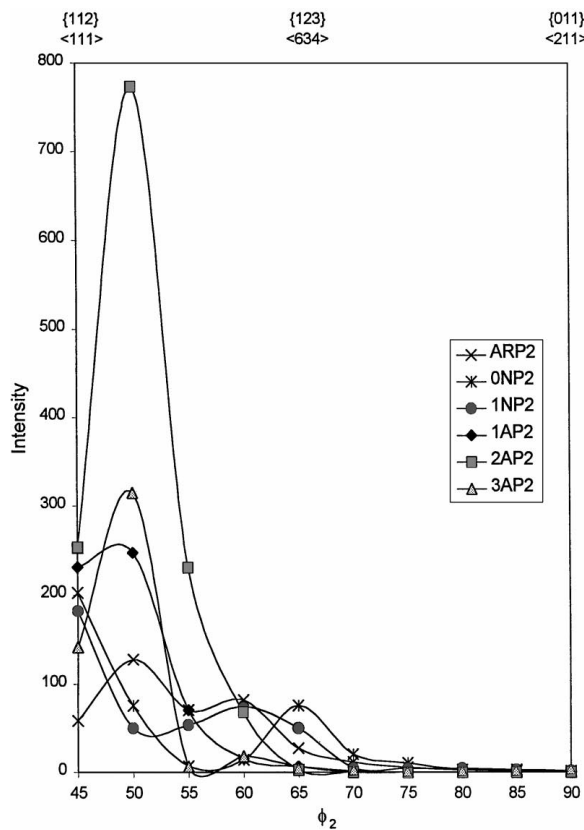


Figure 5 Intensities along the ideal α -fiber. Legend: AR=as received condition, the first numbers 0–3 represent percentage of additional rolling, e.g. 0=0%, 1=10%, etc. N=natural aged condition, A=artificial aged condition, P2 and P4 represent 0.2t position or 0.5t position, respectively.

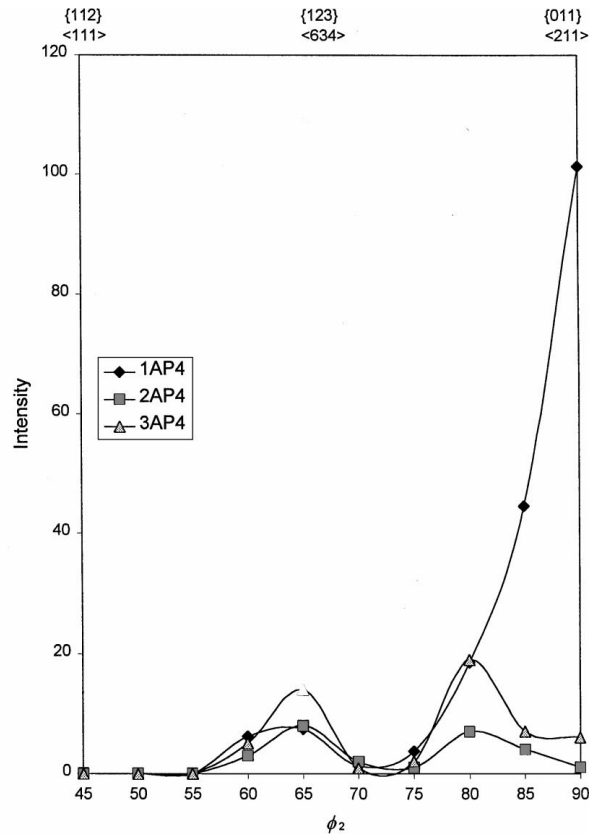
While components describe texture as peak density orientations, texture may also be represented in the form of orientation density along a “fiber” that connects ideal orientations. Fiber representations enable the comparison of measured intensities or other texture “volume” data between materials with different processing histories. The α - and β -fibers are usually identified in FCC alloys. The α -fiber is defined in Bunge notation by the variation of the angle ϕ_1 at constant $\Phi = 45^\circ$ and $\phi_2 = 0^\circ$. It runs from the Goss orientation through the brass orientation to $\{001\}\langle 011 \rangle$. The β -fiber position runs from the Cu orientation, through the S orientation and connects to the α -fiber at the Bs orientation.

The α -fiber is shown in Fig. 5 as the variation of measured intensities along the fiber. Some Al-Li alloys contain elements that inhibit recrystallization [3]. Recrystallization was not expected and no recrystallization texture components were observed. The α -fiber plot shown in Fig. 5 evidences this since the measured intensities are negligible at the Goss recrystallization orientation for all specimens. The intensity values begin to increase at the Bs orientation for the specimens from the 0.5t position, reaching a maximum between $\phi_1 = 45^\circ$ and $\phi_1 = 65^\circ$. Around $\phi_1 = 70^\circ$ the intensity of the 0.5t position samples tapers off to zero while there is a peak observed for the 0.2t samples.

Fig. 6 shows a plot of the intensities along the ideal β -fiber. Locations of the copper, S, and brass components along the fiber are indicated. The intensities at the 0.2t position are significant at the copper and S orientations as shown in Fig. 6a. The measured intensity at the copper orientation is least for the as-received



(a)



(b)

Figure 6 Intensities along the ideal β -fiber. Legend: AR = as received condition, the first numbers 0–3 represent percentage of additional rolling, e.g. 0 = 0%, 1 = 10%, etc. N = natural aged condition, A = artificial aged condition, P2 and P4 represent $0.2t$ position or $0.5t$ position, respectively. (a) $0.2t$ position. (b) $0.5t$ position.

specimen. With solutionizing treatment, 0NP2 (no additional rolling) and 1NP2 (10% additional rolling) specimens exhibit measured intensities near the same value, approximately 230 pct. higher than the as received. After artificial aging, the measured intensity with 10% additional rolling (1AP2) increases compared to 1NP2 by approximately 25 pct. Again, in the artificial aged condition, the intensity at the copper orientation increases slightly with another rolling pass (20% additional rolling). However, a third rolling pass (30% additional rolling) appears to degrade the intensity at the copper orientation in the artificial aged condition (3AP2), resulting in an intensity decrease of approximately 45 pct. from the maximum value of 2AP2. At the S orientation, the measured intensities are significant in the as received and the natural aged specimens. Among these three, the as-received S orientation intensity is the least, it increases nearly 200 pct. with solutionizing treatment, without additional rolling. After 10% additional rolling (1NP2), the measured intensity at the S orientation decreases approximately 33 pct. from 0NP2. At the S orientation, the measured intensities are not significant for the artificial aged specimens. At the brass orientation, all measured intensities are negligible for the specimens of Fig. 6a.

Comparatively, for the specimens from the $0.5t$ position shown in Fig. 6b, the measured intensities are negligible at the copper orientation. The measured intensities at the S orientation are on the same scale as

those of the artificial aged specimens in Fig. 6a. The intensity of the center position increases rapidly along the β -fiber from the S orientation to the brass orientation for the artificial aged specimen with 10% additional rolling. However, with a second (2AP4) and third (3AP4) rolling pass, the measured intensity at the brass orientation on the β -fiber is significantly reduced. A fiber is represented in ideal orientations, however the location of the maximum in an orientation distribution may not necessarily be located on the ideal fiber. An increase in deformation may cause a shift away from the ideal. For this reason, the locations of the maximum intensities are sometimes plotted instead of the ideal fibers.

4. Conclusion

The usual texture orientations expected for rolled aluminum alloys were generally observed in the Al-Cu-Li plate material. The copper and S orientations observed in the ODFs from the $0.2t$ through-thickness position are consistent with flat grains as may be predicted using the Taylor relaxed constraints model. The texture gradient is evidenced by comparing ODFs between the $0.2t$ and the $0.5t$ (center) position. At $0.5t$, no copper component or significant S component is visible, whereas brass is the dominant orientation seen. The through-thickness texture variation in the plate is likely due to the differing amounts or modes of deformation

experienced at different positions though the plate. Most of the rolling process is concentrated near the surface of the plate whereas the center of the plate experiences the least amount of the total deformation. Increasing the amount of deformation beyond the as-received condition affects the intensity values along the ideal fibers in the Al-Cu-Li material studied. Increasing deformation does not always signal a corresponding intensity increase. In some cases, the intensity on the fiber decreases with increasing deformation. This may be due to changing modes of deformation with additional deformation.

Acknowledgements

This research was partially supported by the Louisiana Board of Regents with Lockheed Martin Manned Space Systems under the contract LEQSF (1994–97)-ENH-PLEx-05 and through the Louisiana Board of Regents fellowship support for Ms. Crosby. Partial support was also provided by the NASA/LaSPACE grant under account number 127-40-5102. The authors would like to thank Los Alamos National Laboratory, Los Alamos, New Mexico, Materials Science and Technology Division (MST-8) and Center for Materials Research for technical and financial support to complete this research. Special thanks are due to S.-R. Chen, J. Bingert, and C. Necker of LANL for their assistance with texture analysis and also to M. Lopez.

References

1. V. GEROLD, H.-J. GUDLADT and J. LENDVAI, *Phys. Stat. Sol. A* **131** (1992) 1509.
2. E. W. LEE, in "Light Materials for Transportation Systems," edited by N. J. Kim (Center for Advanced Aerospace Materials, 1993) p. 79.
3. K. VASUDEVAN, W. G. FRICKE JR., M. A. PRZYSTUPA and S. PANCHANADEESWARAN, in Proceedings of the Eighth International Conference on Textures of Materials, 1988, edited by J. S. Kallend and G. Gottstein (The Metallurgical Society, Warrendale, PA, 1988) p. 1071.

4. U. F. KOCKS and H. CHANDRA, *Acta Metall.* **30** (1982) 695.
5. J. MIZERA, J. H. DRIVER, E. JEZIERSKA and K. J. KURZYDLOWKI, *Mater. Sci. Eng.* **212A** (1996) 94.
6. A. FJELDLY and H. J. ROVEN, *Acta Mater.* **44** (1996) 3497.
7. H. J. BUNGE, *Int. Mater. Rev.* **32** (1987) 265.
8. R. W. CAHN, in "Materials Science and Technology: A Comprehensive Treatment Vol. 15" (VCH-Verlagsgesellschaft mbH, Weinheim, Germany, 1993), p. 429.
9. M. HATHERLY and W. B. HUTCHINSON, in "Introduction to Textures in Metals" (The Institution of Metallurgists, London, 1979) p. 8.
10. J. S. KALLEND, U. F. KOCKS, A. D. ROLLETT and H. R. WENK, *Mater. Sci. Eng.* **132A** (1991) 1.
11. H. MECKING, in "Preferred Orientation in Deformed Metals and Rocks: An Introduction to Modern Texture Analysis" (Academic Press, Inc., Orlando, 1985) p. 283.
12. A. D. ROLLETT and S. I. WRIGHT, in "Texture and Anisotropy: Preferred Orientations in Polycrystals and their Effect on Materials Properties" (Cambridge University Press, 1998) p. 185.
13. F. BARLAT and O. RICHMOND, *Mater. Sci. Eng.* **95** (1987) 15.
14. H. J. BUNGE, in "Mathematische Methoden der Textureanalyse" (Akademie-Verlag, Berlin, 1969).
15. H. R. WENK and U. F. KOCKS, *Met. Trans.* **18** (1987) 1083.
16. G. SACHS, *Z. Verein Deut. Ing.* **72** (1928) 134.
17. G. I. TAYLOR, *J. Inst. Met.* **62** (1938) 307.
18. *Idem.*, in "Contributions to the Mechanics of Solids" (Macmillan, New York, 1938) p. 218.
19. J. F. W. BISHOP and R. HILL, *Phil. Mag.* **42** (1951) 414.
20. *Idem.*, *ibid.* **42** (1951) 1298.
21. J. HIRSCH and K. LÜCKE, in "Preferred Orientation in Deformed Metals and Rocks: An Introduction to Modern Texture Analysis" (Academic Press, Inc., Orlando, 1985) p. 309.
22. B. SKROTZKI, G. J. SHIFLET and E. A. STARKE, JR., in "SEAS Report No. UVA/538865/MSE95/101" (Dept. of Materials Science and Engineering, University of Virginia, Charlottesville, VA).
23. X.-H. ZENG and F. BARLAT, *Met. Trans. A* **25** (1994) 2783.
24. H. HONNEFF and H. MECKING, in Proc. 5th Int. Conf. On Textures of Materials, edited by G. Gottstein and K. Lucke (Springer, Berlin, 1978) p. 265.
25. H. MECKING, in "Preferred Orientation in Deformed Metals and Rocks: An Introduction to Modern Texture Analysis" (Academic Press, Inc., Orlando, 1985) p. 283.

*Received 1 September
and accepted 7 December 1999*